第4回構造物の破壊過程解明に基づく
地震防災性向上に関するシンポジウム論文集　2003年3月

AN EXPERIMENTAL STUDY ON FAULT RUPTURE PROPAGATION IN SANDY SOIL DEPOSIT

○Jea Woo LEE[1], Ryoichi IWANAGA[2], Go TABUCHI[2] and Masanori HAMADA[3]

[1] Student Member of JSCE, Ph.D. Candidate, School of Science and Engineering, Waseda University
(3-4-1, Ohkubo, Shinjuku-ku, Tokyo, 169-8555、Japan)
[2] Graduate Student, School of Science and Engineering, Waseda University
(3-4-1, Ohkubo, Shinjuku-ku, Tokyo, 169-8555、Japan)
[3] Fellow of JSCE, Dr. of Eng., Professor, School of Science and Engineering, Waseda University
(3-4-1, Ohkubo, Shinjuku-ku, Tokyo, 169-8555、Japan)

1999年に発生したトルコ・コジャエリ地震および台湾・集々地震は，地表地震断層に対する社会基盤構造物の耐震性の問題を提起した．日米両国の研究者により，この課題に関する研究がいくつか行われているが，いまだ未解決な点が多く残っている．著者らは，実験的および解析的手法を用いて，地下断層の変位による砂質地盤中の破壊の伝播を検討した．模型実験では地表での破壊の到達位置が層厚の影響を受けるという従来の研究結果とは異なった結果が得られた．

Key Words : *fault, rupture propagation, surface fault, experiment, numerical analysis*

1. INTRODUCTION

Recent earthquakes occurred at Kocaeli (Mw 7.3, 1999, Turkey) and Jiji (Mw 7.9, 1999, Taiwan) revealed that ground surface ruptures, induced by faulting movement in the underlying bedrock, could cause severe damages to the major infrastructures. Surface rupture along the Chelungpu fault during Jiji earthquake in Taiwan thrust buildings laterally, and racked buildings and industrial facilities such as concrete dam, lifelines due to differential vertical ground movements. Similarly a number of buildings and public facilities were injured from the combination of lateral and vertical movement of surface ground during Kocaeli earthquake in Turkey. In spite of harmlessness owing to the extremely low population in Tibet plateau, Central Kunlun (Ms 8.1, 2001, China) earthquake produced 400 km long surface fault rupture zone, the length and maximum displacement of which is the largest among the surface rupture zones reported on so far. These tragic events invoked us the necessities of proper understanding of fault rupture propagation through soil deposits.

A few of seismic researchers in Japan and US have continuously paid their efforts to examine the complex phenomenon through experimental and analytical studies. Roth et al. (1982) performed a series of centrifugal tests to simulate the rupture propagation of sand under more realistic gravity stress condition. Cole et al. (1984) presented a theoretical model to predict the location of surface rupture based on the results from a series of 1-g fault box tests of alluvial sand. Bray et al. (1994) released the experimental and analytical results of studies on the response of saturated clay soils to bed rock displacement. Several series of 1-g fault box test using Toyoura sand and silica sand in dry were carried out to investigate the effect of fault type on the required displacement to form shear rupture by Tani et al. (1994, 1999), who also suggested the modified analytical model to predict the behavior of rupture propagation based on their experimental studies.

In this study a series of model test for dip-slip faulting using 1-g fault test box has been conducted to examine the rupture propagation in dry sand with particular concern on the relationship between the fault type and the affecting factors required to develop complete shear ruptures to ground surface. An improved testing device was prepared to minimize sorts of possible errors during the test. The results from numerical simulation utilizing elasto-plastic theory and finite difference scheme additionally present an appropriate agreement with the experimental results.

2. SETUP AND PROCEDURE FOR 1-G FAULT RUPTURE TEST

(1) Preparation of Testing Apparatus

Two kinds of testing devices, similar to them used by Cole et al. (1984) and Tani et al. (1994), have been introduced to conduct the dip-slip faulting tests under 1-g condition. Both of the devices are not identical in dimension and configuration but have been designed to function in the same way. The earlier-made device (Apparatus I, **Fig. 1 (a)**) was molded with steel frame and acrylic board-walled box of which dimension is 2.0m-0.5m-1.0m in length, width and depth. And a hand-operated hydraulic jack was used to activate the up and down movement of bottom plate in the apparatus.

On the contrary Apparatus II (**Fig. 1 (b)**) built up using a lager glass-walled box of which dimension is 3.0m-1.0m-1.0m in length, width and depth, one-half of its basal plate could be moved up or down along various angles to relative to the fixed half using a electronically controlled high-capacity motor. The adjustable rolling hopper was also assembled to place the sand in the testing box at a uniform density, whereas it was not available to the earlier device. **Fig. 1** explains the details of updates of the improved device.

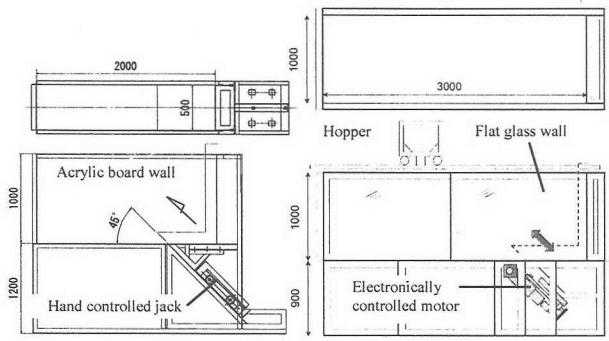

(a) Apparatus I **(b)** Apparatus II

Fig. 1 Testing devices used in 1g-fault test

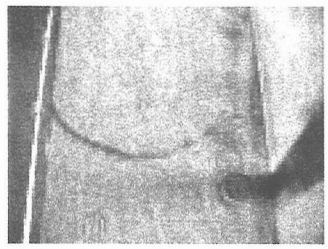

Fig. 2 Half-moon shape of surface rupture due to wall friction

While performing sorts of tests using Apparatus I, some of troubles such as the leakage of sand, unexpected shape of failure line and the effect of wall friction were encountered. The most serious one among them was thought to be the effect of wall friction which was regarded to be caused by relatively narrow width of testing box and high level of frictional resistance between acrylic board wall and soil mass comparing with case of glass wall. Since this effect is apt to form a distorted pattern of deformation as shown **Fig. 2**, it makes it difficult to measure the exact location of rupturing point on the surface of soil mass.

It is shown that this problem can be effectively avoided by the use of the glass walled box and sufficient width of testing box for the apparatus, as the experimental results form the improved testing apparatus presents no significant evidence of wall friction such as a configuration similar to a half moon shape of failure surface. (Refer to **Fig. 3 (c)**)

(2) Specimen for Test

Basically the specimen used in the experiments is divided into dense and loose granular materials. Silica sand of which D_{50} - that corresponds to the grain size 50% finer - is 0.157mm, was placed in the apparatus at a uniform densities for dense/loose state - its relative density, D_r is about 83±4%, 59±4% respectively - by raining itself into the box with the adjustable hopper. Several number of laboratory tests using small-size aluminum can have been performed to measure the density of sand for each case. The soil parameters related to grain size are summarized in **Table 1**.

Table 1 Soil parameters used in tests

Material Type	Silica Sand No. 7
Average Grain size D_{50}	0.157mm
Uniformity Coefficient Uc	1.55
Coefficient of Curvature Uc'	0.946
Relative Density Dr	Loose : 59±4% Dense : 83±4%

(3) Testing Procedure

The procedure for 1-g fault test in this study consists of stepwise movement of basal deck of the testing device. The details of the procedure for each faulting angle are summarized as bellows;

i) Preparation of uniform sand layer using hopper with installation of black sand grid and target, ii) Activation of up/down movement of deck to the every incremental displacement with constant speed of 2mm/min., iii) Taking photos of both sides of deformed specimen and surface of soil mass at every increment of vertical displacement, iv) Repetition of processes described as ii) and iii) to required offset to form complete shear ruptures.

(4) Testing Cases

Totally 22 cases of experiments were conducted with variation of height of soil layer and dip angle

for loose/dense sand. As for a dense/loose sand layer with the height of 20cm, 3 cases of dip angle ranging as 30°, 45° and 60° were implemented. The effect of height of soil layer was evaluated from the tests on dense sand of which thickness varies from 10cm to 60cm with dip angle 45°.

3. OBSERVED BEHAVIOR FROM TEST

(1) Rupture Pattern Induced by Dip-slip Fault

Propagation of shear failure through sandy soil mass can be obviously seen the successive three photographs shown in **Fig. 3 (a)**. The shape of failure surfaces due to dip-slip (up and down) movement of basal plate appeared similar to the results previously presented by Cole et al. (1984) and Tani et al. (1996) in general. As shown in **Fig 3 (a)**, the failure surfaces for all reverse faults initiate from the contact of the soil mass and movable bottom plate approximately tangent to the fault dip angle. And they gradually move to outward from the initiating point, then finally shape the curve that can be represented by logarithmic spiral.

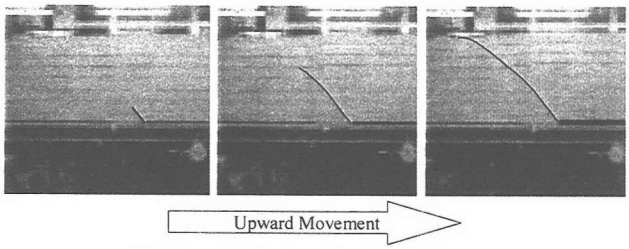

(a) Reverse fault - side view, H=40cm

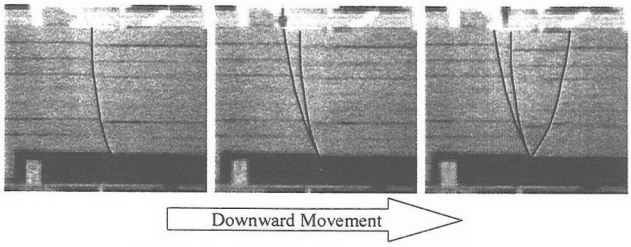

(b) Normal fault - side view, H=40cm

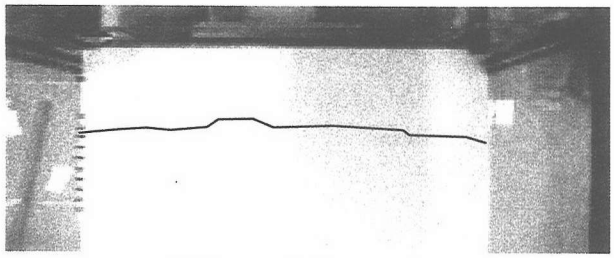

(c) Reverse fault - over view
(shape of surface rupture is almost straight)

Fig. 3 Selected photos corresponding to three stages in reverse /normal faulting test on dense sand with dip angle=45°

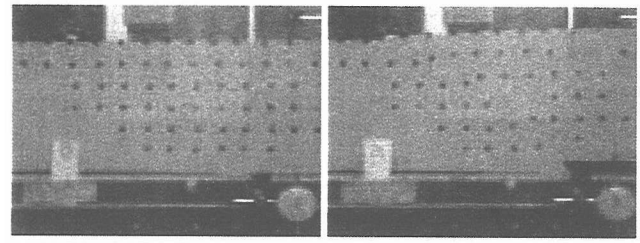

(a) Vertical Offset 0mm **(b)** Vertical Offset 25mm

Fig. 4 Development of fault rupture with targets for image processing

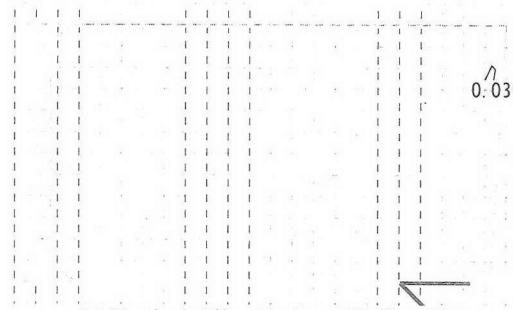

(a) Vertical Offset D=1mm (D/H=0.3%)

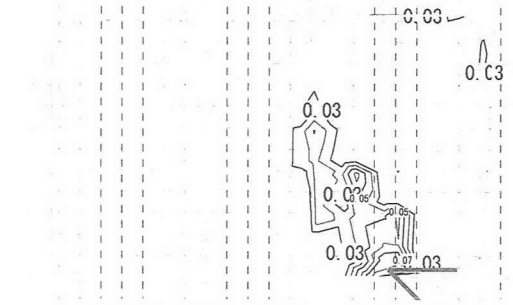

(b) Vertical Offset D=8mm (D/H=2.7%)

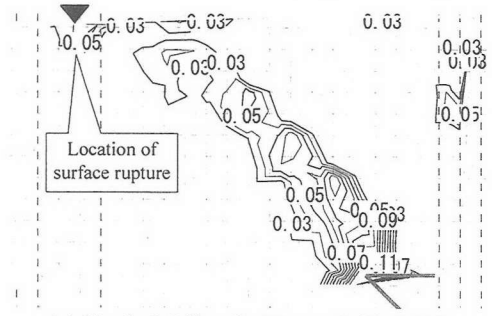

(c) Vertical Offset D=12mm (D/H=4.0%)

Fig. 5 Acquisition of maximum shear strain contour using image processing

As for the failure surfaces developed by normal faults, three lines of failure surfaces were taken place successively as the fault displacement continued, which is also close to the previous experimental results presented by Cole et al. (1984) and Tani et al. (1996). However, Cole et al. classified order, and Tani et al. suggested four stages of development for the failures, whereas this study divided them by 3 categories. As shown in **Fig. 3 (b)**, the first failure surface began to propagate directly up to the surface regardless to dip angle, a bit of continuous movement of basal plate formed the

second failure surface in the fore side, then finally the third failure surface developed in opposition to preceded two surfaces, as the continuous faulting configured complete shear band.

The contours of maximum shear strain at the moment of initial appearance of surface failure were achieved using a digital processing software being capable of capturing the relative displacements of targets installed in soil model. (Refer to **Fig. 4**)

Based on the achieved increments of displacement at grid points, the maximum shear strain can be calculated using simple equations prevailed in the area of engineering mechanics. **Fig. 5** shows the distribution of maximum shear strain contours corresponding to the propagation of failure surface. As shown in the **Fig. 5 (c)**, it was found that the normalized vertical displacement, denoted by D/H, was equal to 4.0% as the failure surface initiating from the bottom of the soil model reached the surface of the model. At the same time, referring to the measured location of surface rupture - marked as reverse triangle in **Fig. 5 (c)**- from the fault box test, the value of maximum shear strain equivalent to the failure surfaces was appeared to be 0.03 when the complete failure surfaces initially constituted in soil mass.

(2) Location of Surface Rupture

Based on the testing results described in the previous section, a model for observation of rupture pattern is depicted as **Fig. 6**. Referring to the model, the relationship of the horizontal distance, W, of the rupture surface from the point on the surface vertically above the point where the fault intersects the bottom of the sand mass and its affecting factors involving the faulting dip angle θ, the height of the soil mass H, can be explained as shown in **Fig. 7**.

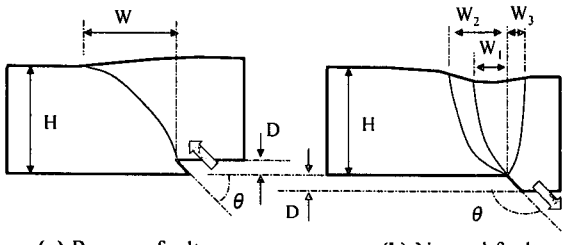

(a) Reverse fault (b) Normal fault

Fig. 6 Model for the evaluation of rupture patterns

Fig. 7 (a) and **(b)** illustrates the variation of W/H and D/H according to the changes of dip angle. For the reverse faults, there happened relatively stiff inclination of the value of W/H to down with increase of the dip angle, but there is only a little change in value for the normal faults. On the contrary, there is a reverse tendency in the variation of D/H. It appeared to be very significant in case of the normal faults, whereas there is only a slight variance in D/H for the reverse faults.

Regarding the effect of height of soil layer, **Fig. 7 (c)** shows that the distance W is coming closer to the point the fault intersects with increase of the height of soil mass. This implies that the rupture pattern changes as the thickness of the soil mass is varied. Besides, it can be seen in **Fig. 7 (d)** that a complete failure surface forms in dense sand mass at a normalized vertical displacement of approximately 4~5% with reverse faulting. And it is also found that the vertical displacement required to form complete shear failure in loose sand mass is approximately 7.0~7.5%, which is greatly larger than that required in dense sand mass.

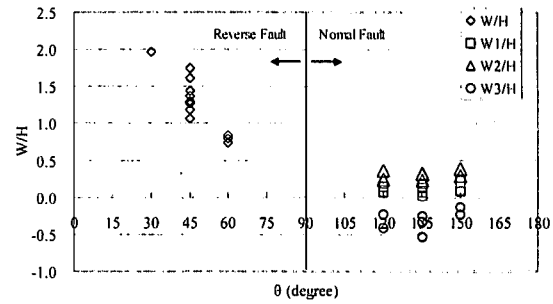

(a) W/H versus θ

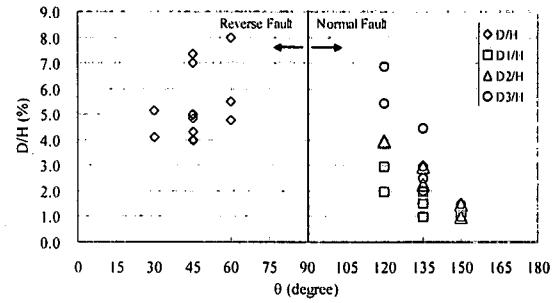

(b) D/H versus θ

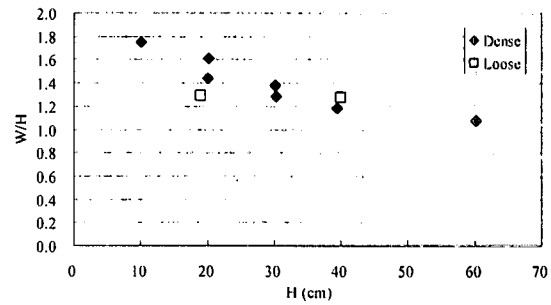

(c) W/H versus H (Reverse fault with θ=45°)

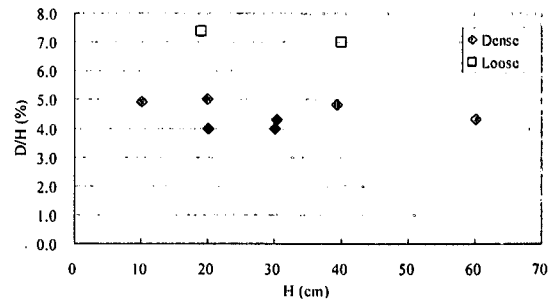

(d) D/H versus H (Reverse fault with θ=45°)

Fig. 7 Variation of W/H and D/H as a function of θ and H

4. NUMERICAL SIMULATION

(1) Numerical Model

Several cases of numerical analysis have been performed to investigate the response of alluvial soil subjected to dip-slip faulting movement using FLAC Ver. 3.3 (Itasca, 1995). Mohr-Coulomb failure criterion is adopted to allow for the simulation of plastic behavior of the model. And the Lagrangian scheme in which the coordinate of each grid is updated according to the development of plastic increment is utilized to minimize the calculating shock responding to the progress of plastic large deformation. The material properties of the sand used in 1g-Fault Box test were obtained from a series of confined compressive tests (CD) as shown in **Table 2**.

Table 2 Material Properties used in FLAC Analysis

Items	Unit Weight γ, (ton/m^3)	Elastic Modulus E, (Mpa)	Friction Angle ϕ, (°)	Poisson Ratio ν
Value	1.435	67.56	34.12 (Residual Strength)	0.36

(2) Results from Numerical Analysis

15 cases of fault rupture propagation have been simulated in accordance to the variation of dip angle of basement fault and height of a sandy soil (c=0.0). **Fig. 8** demonstrates an example of the deformed meshes resulted from the cases with vertical offset as much as 10% of height of soil layer regarding dip angle of 60°. The calculated W/H according to the variation of height of the soil layer is depicted in **Fig. 9**. The value of W was measured form the distribution of calculated maximum shear strain in soil mass. As shown in **Fig. 9**, on the contrary to the results from 1g-fault box tests presented in **Fig. 7 (c)**, the value of the ratio W/H with respect to 45 degree of dip angle shows no variation regarding the increase of height of soil layer. The results form the case of 60 degree of sip angle also presents no definite trends as to the variation of dip angle. But with respect to 30 degree of dip angle, the value of the ratio W/H tends to be getting greater according to the increase of height of soil layer. This tendency somewhat differ from the experimental results that show certain decrease of W/H in accordance with the increase of height of soil mass, even if the tests were limited to the 45° of dip angle. It can be inferred from the results from numerical simulations that with assumption that the material properties of soil mass is not changed depending upon confining stress, the height of soil mass little affects the location of the surface rupture at least where the dip angle is stiffer than 45°.

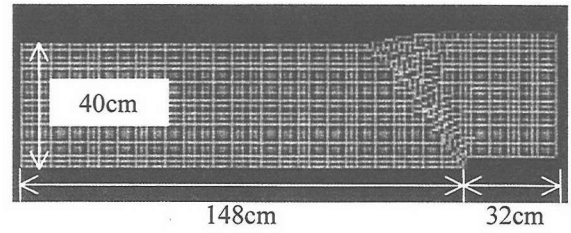

Fig. 8 Deformed Mesh, D/H=10%, Dip angle=60°

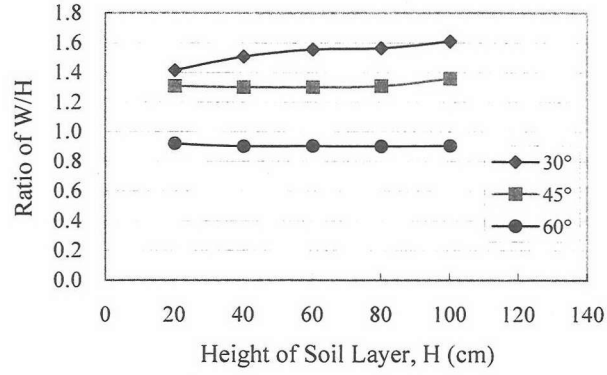

Fig. 9 W/H versus Height of soil layer from numerical analysis

5. DISCUSSION

(1) Comparison with the Results from Numerical Simulation

As described in the previous section, numerical analyses using FDM and Mohr-Coulomb failure criterion have been implemented to verify the experimental results in this study. By means of the digital processing of the experimental data, it was acquired that the complete slip line developed in fault box model appropriately coincide with a contour of maximum shear strain with value of 0.03 in soil mass with faulting angle of 45°. Thus, it is worthwhile comparing the experimental results and the results form numerical simulations to validate a tendency of the soil behavior achieved from the fault box tests.

The maximum shear strain in FLAC is defined as the following equation, which is same as one used in the digital processing of the experimental results.

$$\gamma = \frac{1}{2}\sqrt{(\varepsilon_{xx} - \varepsilon_{yy})^2 + 4\varepsilon_{xy}{}^2}$$

Fig. 10 shows the distribution of calculated maximum shear strain lized vertical displacement to develop a complete slip line in dense sand mass. Comparing with the experimental results shown in **Fig. 5**, the entire feature of calculated maximum shear strain contours in numerical model subjected to reverse faulting with dip angle of 45° show good agreement measured one from the 1g-faul box tests.

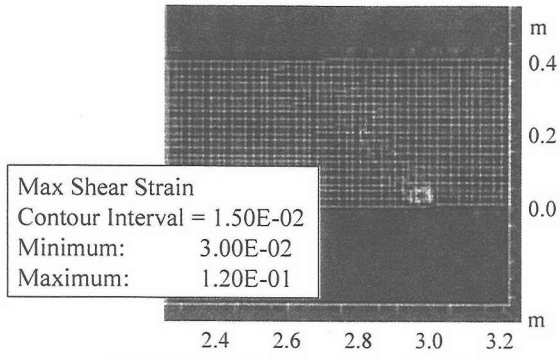

(a) D/H=2%, H=40cm, dip angle=45°

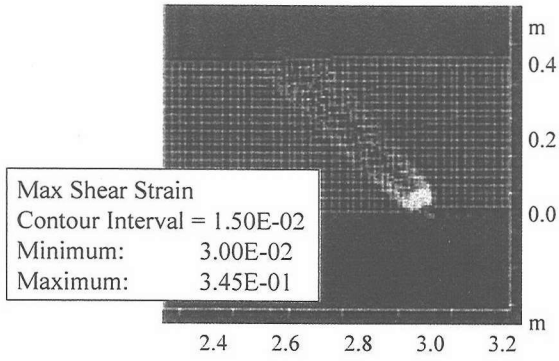

(b) D/H=4%, H=40cm, dip angle=45°

Fig. 10 Calculated maximum shear strains in dense sand

(2) Comparison with the Previous Studies

Comparison with the experimental results and the theoretical model presented by Tani et al. (1996) invokes much of attention to understanding of the experimental results in this study. Tani et al. (1999) suggested a modified theoretical model to predict the location and pattern of faulting rupture based on their experimental results. **Fig. 11** presents a diagram in which the author's experimental results, Tani et al's experimental results and calculated values by Tani's modified model have been plotted altogether. It can be obviously seen that there is a significant dispersion in the experimental results of Tani et al's, whereas a distinct tendency inclining to down in value of W/H corresponding to the height of soil mass. Considering Tani et al's comment that the features of fault rupture propagation in model tests are basically identical with various heights of sand layers, the author's founding in this study is somewhat exceptional and noticeable.

Bray et al. (1996) noticed that the angle of dilation of sand under low confinement could differ from that in the larger prototype earth structures. Moreover, the volume change tendencies of dry sand can very significantly at low confining stress as the thickness of sand in 1g-fault box test is varied. Therefore, given the demonstrated importance of dilation angle of sand and the experimental results come out from this study, it would be reasonable to yield the declining tendency with increase of the height of sand mass in 1-g fault box test.

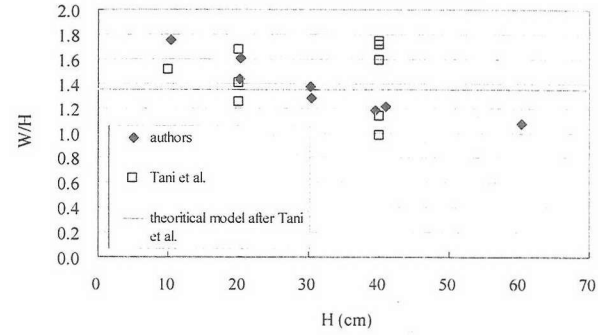

Fig. 11 Comparison of experimental results with Tani et al.'s

6. CONCLUSION AND FUTURE STUDIES

The patterns and the location of fault rupture in a sandy soil overlying active dip-slip fault have been studied on the basis of the results from 1-g fault box tests and numerical simulation.. The relationship of the location of surface rupture and its affecting factors were also evaluated. By the comparison with previous studies, the experimental results and their trends in this study were turned out to be consistent with them on the whole except that change of rupture pattern with various height of soil mass. For further understanding of the phenomenon, it should be followed to carry out the experiments in various conditions of sandy soils. Considering the tendency achieved from this study, it is strongly needed to verify the effect of thickness of soil mass on the development of rupture pattern. The centrifugal tests for simulation of dip slip faulting will be thus performed by the authors to investigate the effect of confining stress in sandy soil mass in near future.

REFERENCES

1) Bray, J. D., Seed, R. B., and Seed, H. B., Analysis of earthquake fault rupture propagation through cohesive soil, *Journal of Geotechnical Engineering,* ASCE, Vol. 120, No 3., pp. 562-580, 1994
2) Bray, J. D., Developing mitigation measures for the hazards associated with earthquake surface fault rupture, *Proceedings of A Workshop on Seismic Fault-Induced Failures* pp. 55-77, 2001
3) Cole, D. A., Jr., and Lade, P. V., Influence zones in alluvium over dip-slip faults. *Journal of Geotechnical Engineering*, ASCE, Vol. 110, No. GT5, pp. 599-615, 1984
4) Lazarte, C. A., The response of earth structures to surface fault rupture, *PhD thesis*, University of California at Berkeley, Berkeley, CA, United States, 1996
5) Hamada, M., Research subjects on earthquake resistance of civil infrastructures against fault-induced ground surface ruptures, *Proceedings of A Workshop on Seismic Fault-Induced Failures* pp. 131-134, 2001
6) Tani, K., Ueta, K. and Onizuka, N., Scale effect of quaternary ground deformation observed in model tests of vertical fault, *Proceeding of 29th Japan National Conference on SMFE*, pp. 1359~1362, 1994 (in Japanese)